Author Manuscript

Author Manuscript

Author Manuscript

Author Manuscript

HHS Public Access

Author manuscript

Brain Behav Immun. Author manuscript; available in PMC 2020 October 01.

Published in final edited form as:

Brain Behav Immun. 2019 October ; 81: 151–160. doi:10.1016/j.bbi.2019.06.008.

Treatment with a heat-killed preparation of *Mycobacterium vaccae* after fear conditioning enhances fear extinction in the fear-potentiated startle paradigm

James E. Hassell Jr.[a,b], **James H. Fox**[a], **Mathew R. Arnold**[a,b], **Philip H. Siebler**[a], **Margaret W. Lieb**[a], **Dominic Schmidt**[a], **Emma J. Spratt**[a], **Tessa M. Smith**[a], **Kadi T. Nguyen**[a], **Chloé A. Gates**[a], **Kaley S. Holmes**[a], **K'loni S. Schnabel**[a], **Kelsey M. Loupy**[a], **Maike Erber**[c], **Christopher A. Lowry**[a,b,d,e,f,*]

[a]Department of Integrative Physiology, University of Colorado Boulder, Boulder, CO 80309-0354, USA

[b]Center for Neuroscience, University of Colorado Boulder, Boulder, CO 80309-0354, USA

[c]Laboratory for Molecular Psychosomatics, Clinic for Psychosomatic Medicine and Psychotherapy, University of Ulm, D-89081 Ulm, Germany

[d]Department of Physical Medicine & Rehabilitation and Center for Neuroscience, University of Colorado Anschutz Medical Campus, Aurora, CO, 80045, USA

[e]Rocky Mountain Mental Illness Research Education and Clinical Center, Aurora, CO 80220, USA

[f]Military and Veteran Microbiome Consortium for Research and Education (MVM-CoRE), Aurora, CO 80220, USA

Abstract

The hygiene hypothesis or "Old Friends" hypothesis proposes that inflammatory diseases are increasing in modern urban societies, due in part to reduced exposure to microorganisms that drive immunoregulatory circuits and a failure to terminate inappropriate inflammatory responses. Inappropriate inflammation is also emerging as a risk factor for anxiety disorders, affective disorders, and trauma-and stressor-related disorders, including posttraumatic stress disorder (PTSD), which is characterized as persistent re-experiencing of the trauma after a traumatic experience. Traumatic experiences can lead to long-lasting fear memories and fear potentiation of the acoustic startle reflex. The acoustic startle reflex is an ethologically relevant reflex and can be potentiated in both humans and rats through Pavlovian conditioning. *Mycobacterium vaccae* is a soil-derived bacterium with immunoregulatory and anti-inflammatory properties that has demonstrated to enhance fear extinction in the fear potentiated startle paradigm when given prior to fear conditioning. To determine if immunization with *M. vaccae* after fear conditioning also has

[*]**Corresponding author**: Christopher A. Lowry, Department of Integrative Physiology and Center for Neuroscience, University of Colorado Boulder, Boulder, CO 80309-0354, USA, Tel (303) 492 – 6029, Christopher.Lowry@colorado.edu.

Publisher's Disclaimer: This is a PDF file of an unedited manuscript that has been accepted for publication. As a service to our customers we are providing this early version of the manuscript. The manuscript will undergo copyediting, typesetting, and review of the resulting proof before it is published in its final citable form. Please note that during the production process errors may be discovered which could affect the content, and all legal disclaimers that apply to the journal pertain.

Author Manuscript Author Manuscript Author Manuscript Author Manuscript

protective effects, adult male Sprague Dawley rats underwent fear conditioning on days −37 and −36 followed by immunizations (3x), once per week beginning 24 h following fear conditioning, with a heat-killed preparation of *M. vaccae* NCTC 11659 (0.1 mg, s.c., in 100 μl borate-buffered saline) or vehicle, and, then, 3 weeks following the final immunization, were tested in the fear-potentiated startle paradigm (n = 12 per group). Rats underwent fear extinction training on days 1 through 6 followed by spontaneous recovery 14 days later (day 20). Rats were euthanized on day 21 and brain tissue was sectioned for analysis of *Tph2, Htr1a*, *Slc6a4*, *Slc22a3,* and *Crhr2* mRNA expression throughout the brainstem dorsal and median raphe nuclei. Immunization with *M. vaccae* did not affect fear expression on day 1. However, *M. vaccae*-immunized rats showed enhanced between-session and within-session extinction beginning on day 2, relative to vehicle-immunized controls. Immunization with *M. vaccae* and fear-potentiated startle had minimal effects on serotonergic gene expression when assessed 42 days after the final immunization. Together with previous studies, these data are consistent with the hypothesis that immunoregulatory strategies, such as immunization with *M. vaccae*, have potential for both prevention and treatment of trauma- and stressor-related psychiatric disorders.

Graphical Abstract

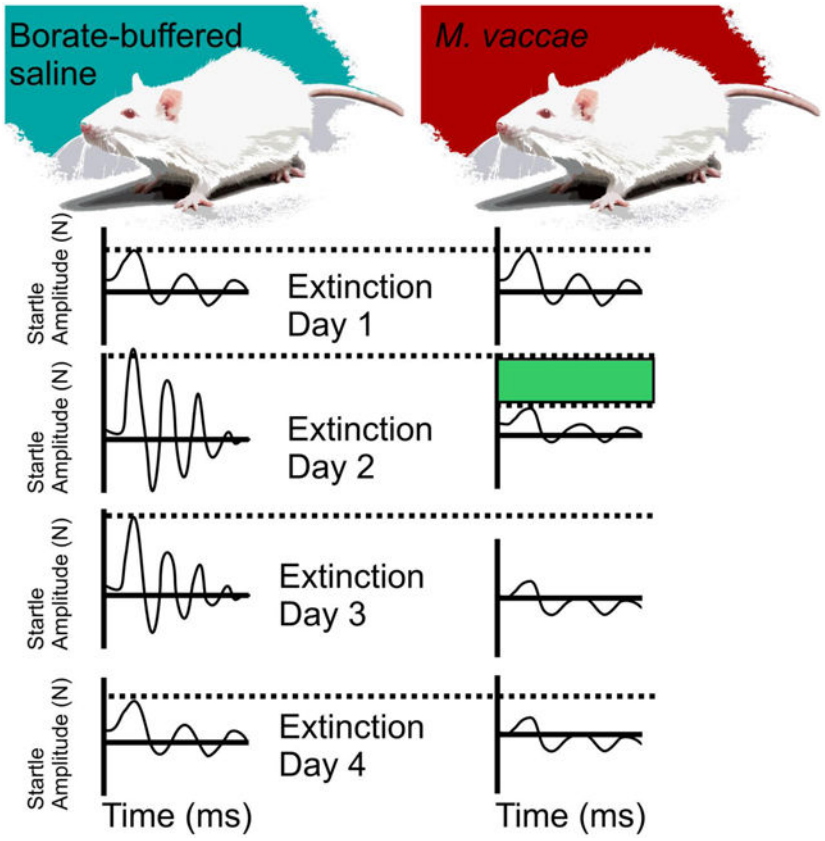

Keywords

dorsal raphe; extinction; fear-potentiated startle; posttraumatic stress disorder; serotonin

Author Manuscript Author Manuscript Author Manuscript Author Manuscript

1. Introduction

Lifetime prevalence of posttraumatic stress disorder (PTSD) is approximately 8.9% in the United States using the *Diagnostic and Statistical Manual of Mental Disorders* (DSM-5) criteria (Kilpatrick et al., 2013). A systematic review of randomized clinical trials for treatments for PTSD revealed that selective serotonin reuptake inhibitors had response rates that range from 17%-85% for treatment of PTSD (Ipser and Stein, 2012). This finding suggests that current treatments for PTSD are variable in response rates and that serotonin systems may be involved in PTSD symptomology.

Support for serotonin involvement in the etiology and pathophysiology of PTSD comes from studies demonstrating that single nucleotide polymorphisms of tryptophan hydroxylase (TPH) 1 (rs2108977) and 2 (rs11187997), rate-limiting enzymes for serotonin synthesis, were found to be associated with PTSD symptoms (Goenjian et al., 2012; Goenjian et al., 2015). Serotonin is also involved in animal models of anxiety (Ren et al., 2018) and fear conditioning (Johnson et al., 2015) (for review, see, (Bocchio et al., 2016; Hassell et al., 2018). Serotonin neurons in areas of the brain such as the dorsal raphe nucleus (DR), an area of the brain that gives rise to the majority of ascending serotonergic projections to forebrain corticolimbic structures, were found to be activated in a fear-potentiated startle (FPS) paradigm (Spannuth et al., 2011). Fear conditioning and fear extinction models such as FPS are useful tools in understanding stress-related disorders such as PTSD (VanElzakker et al., 2014).

Paradigms such as FPS have been used to investigate neural mechanisms of fear-related processes such as fear acquisition (Davis and Astrachan, 1978), between-session fear extinction (Falls et al., 1992), and within-session fear extinction (Davis et al., 1993). Extinction training is a form of inhibition of fear through a process of new learning (Myers et al., 2011; Rescorla, 2004). Individuals diagnosed with PTSD demonstrate a resistance to between-session extinction (Milad et al., 2009) as well as within-session extinction in a symptom severity dependent manner, with individuals with more severe symptoms of PTSD having more resistance to within-session extinction (Norrholm et al., 2011). Individuals with a diagnosis of PTSD and high severity of symptoms were unable to inhibit FPS in the presence of a safety signal (Jovanovic et al., 2009), suggesting that the neurocircuitry involved in inhibition of fear responses is dysregulated. In individuals diagnosed with PTSD with highest severity symptomology, a lack of inhibition of fear, as assessed in an FPS paradigm, has been proposed to differentiate between major depressive disorder and PTSD (Jovanovic et al., 2010).

Inflammatory markers such as interleukin (IL) 6 have been found to be elevated in individuals diagnosed with PTSD (Guo et al., 2012; Lindqvist et al., 2017a; Lindqvist et al., 2014). Additionally, white blood cell count is also higher in individuals diagnosed with PTSD suggesting an increase in immune cell activation (Lindqvist et al., 2017b). Specifically, T-cell populations such as $CD45RA^{-}$ $CCR7^{-}$ effector memory T-cells (Tern) were increased while $CD4^{+}CD25^{+}Foxp3^{+}$ Treg cells were decreased in individuals with PTSD (Sommershof et al., 2009). In a separate study Morath et al. (2014), found that individuals diagnosed with PTSD that underwent Narrative Exposure Therapy had reduced

Author Manuscript Author Manuscript Author Manuscript Author Manuscript

Clinician Administered PTSD scores (CAPS) 4 months after therapy (Morath et al., 2014). Increases in Treg were found to correlate with reduced CAPS scores suggesting that immunoregulation to be involved in decreases in PTSD symptoms (Morath et al., 2014).

Immunizations with a heat-killed preparation of the saprophytic bacterium, *Mycobacterium vaccae* NCTC 11659, in mice exposed to chronic subordinate colony housing (CSC) stress, a murine model of PTSD (Reber et al., 2016a), induces a stress resilient phenotype (Reber et al., 2016b). *M. vaccae* prevented the stress-induced increase in secretion of IL-6 from mesenteric lymph node cells stimulated with anti-CD3 antibody *ex vivo* (Reber et al., 2016b). The protective effects of *M. vaccae* were prevented by pretreatment with an anti-CD25 antibody suggesting that *M. vaccae*'s protective effects were Treg-dependent (Reber et al., 2016b). In other previous studies, immunizations with *M. vaccae* prior to fear conditioning found enhanced between-session and within-session fear extinction (Fox et al., 2017; Loupy et al., 2018). Additionally, serotonergic genes and genes that control serotonergic signaling within the DR such as *Tph2, Htr1a*, and *Slc22a3* and *Crh*, *Crhr1*, and *Crhr2* genes in forebrain areas such as the central nucleus of the amygdala and bed nucleus of the stria terminalis were altered in animals that received *M. vaccae* immunizations that underwent FPS (Fox et al., 2017; Loupy et al., 2018). Therefore, treatments that can modulate serotonergic systems, lower inflammation or induce Treg are of interest for PTSD, anxiety- and fear-related disorders (Langgartner et al., 2019; Michopoulos et al., 2017).

In the current study, we hypothesized that *M. vaccae* immunizations after fear conditioning in a FPS paradigm would enhance between-session and within-session fear extinction. Additionally, we hypothesized that *M. vaccae* immunization after fear conditioning would modulate expression of serotonergic genes and genes that control serotonergic signaling within the DR.

2. Materials and Methods

2.1. Animals

Adult male Sprague Dawley® rats (Strain code 400, Crl:SD; Charles River, Wilmington, MA, USA) weighing 72-111 g (27-32 days old upon arrival) were pair-housed in standard polycarbonate rat cages (26 cm width × 47.6 cm length × 20.3 cm height; Alternative Design, Siloam Springs, AR, USA) containing an approximately 2.5 cm-deep layer of bedding (Cat. No. 7090; Teklad Sani-Chips; Harlan Laboratories, Indianapolis, IN, USA). This species, strain, and supplier were chosen for studies of FPS due to the extensive previous research conducted with these animals using this model (Davis, 1986; Fox et al., 2017). All rats were kept under standard laboratory conditions (12-h light/dark cycle, lights on at 0600 h, 22 °C) and had free access to tap water and standard rat diet (8640 Teklad 22/5 Rodent Diet, Harlan Laboratories). Cages were changed once per week. All studies were consistent with the National Institutes of Health *Guide for the Care and Use of Laboratory Animals, Eighth Edition* (The National Academies Press, 2011) and the Institutional Animal Care and Use Committee at the University of Colorado Boulder approved all procedures. All possible efforts were made to minimize the number of animals used and their suffering.

Author Manuscript Author Manuscript Author Manuscript Author Manuscript

2.1.1. Reagents—These studies used whole heat-killed *M. vaccae* National Collection of Type Cultures (NCTC) 11659 suspension [10 mg/ml solution, diluted to 1 mg/ml in 100 μl sterile borate-buffered saline (BBS), batch ENG#1, provided by BioElpida (Lyon, France)].

2.1.2. *M. vaccae* and vehicle immunization—Experimental rats received either subcutaneous (s.c.) immunization with 0.1 mg whole heat-killed *M. vaccae* suspension or received injections of 100 μl of the vehicle, sterile BBS, using 21-gauge needles and injection sites between the scapulae. The dose used in these experiments (0.1 mg) was 1/10 of the dose used in human studies (1 mg) (O'Brien et al., 2004) and identical to the dose used in previous studies in mice (Lowry et al., 2007; Reber et al., 2016b; Siebler et al., 2018) and rats (Fonken et al., 2018; Frank et al., 2018a; Loupy et al., 2018).

2.1.2.1. General experimental procedures: After arrival (Day −44) rats ($N = 24$) were housed in pairs assigned to receive subcutaneous injections of *M. vaccae* while the other half were housed in pairs assigned to receive subcutaneous injections of BBS vehicle on days −35, −28, and −21. Sample sizes were 1) BBS vehicle ($n = 12$), 2)*M. vaccae* ($n = 12$). We chose to initiate the immunization protocol on day – 35 days of the protocol in order to approximate the timing between the immunization protocol and behavioral testing in a previous study of the ability of *M. vaccae*, when given before fear conditioning, to enhance fear extinction (Fox et al., 2017). In this previous study, we also immunized rats beginning on day −35 of the protocol. The selection of timing for immunizations in the study by Fox and colleagues was in turn based on the timing of immunization in previous studies in mice (Reber et al., 2016b). In Reber et al., 2016, behavioral testing for anxiety-like defensive behavioral responses in the elevated plus-maze was done 39 days after the initial immunization with *M. vaccae* or vehicle. In Fox et al., 2017, extinction training likewise was initiated 39 days following the initial immunizations with *M. vaccae* or vehicle (i.e., after two days of baseline acoustic startle testing and two days of fear conditioning). In the present study, as we did not include baseline acoustic startle testing or fear conditioning immediately before extinction testing, extinction training was initiated 35 days following the initial immunizations with *M. vaccae* or vehicle. The stress resilience effects of *M. vaccae* are thought to be dependent in part on induction of Treg (Reber et al., 2016b), and the half-life of Treg in C57BL/6 mice is 27 days (Depis et al., 2016), which may explain the long-lasting stress resilience effects of*M. vaccae* in different models.

2.1.2.2. Startle apparatus: The apparatus used consisted of a darkened sound-attenuated chamber (35.6 cm width × 27.6 cm depth × 49.5 cm height; SM100SP StartleMonitor Cabinet/Service Pack; Kinder Scientific, Poway, CA, USA). Inside the chamber was an aluminum base plate (Kinder Scientific) connected to a grounding cable to reduce electrical noise. An animal sensing plate for rats (SM2001; Kinder Scientific) was mounted onto the base plate, and contained a piezoelectric transducer. The transducer measured the startle response by converting the mechanical displacement of the animal sensing plate caused by the rat's startle response into a voltage output, which was then amplified, presented to a 12-bit analog-to-digital (A/D) converter and recorded in newtons (N). Startle amplitude was defined as the maximum voltage output during the first 250 msec following each noise burst

Author Manuscript Author Manuscript Author Manuscript Author Manuscript

or during the first 500 msec after the onset of each noise burst during a conditioned stimulus present (CS+) trial. The transducer was calibrated prior to baseline and once again before the first FPS testing session using a Newton Impulse Calibrator (SMCAL; Kinder Scientific). The full-scale setting was determined experimentally so that the maximum startle response reached no more than 75-80% of the full-scale setting. An animal restrainer (9.5 cm width × 17.8 cm length × 17.8 cm height) was placed on top of the animal sensing plate. The animal restrainer had an adjustable ceiling that was positioned so the rat had adequate headroom but was unable to rear. This offered the added benefits of reducing the aversiveness of testing, while minimizing excessive movement. The ceiling level remained at the same height for the duration of FPS training and testing. The rat restrainer also contained 4 stainless steel bars (21.6 cm length; 0.6 cm diameter; 1.3 cm between each bar) used to deliver scrambled foot shocks (0.6 mA, 0.5 sec) that were generated by a Dual Programmable Shocker (scrambled output; DSCK-D; Kinder Scientific). The sound-attenuated chamber also contained a light bulb located 10 cm above the rat restrainer that was used to deliver the conditioned stimulus (CS) and two speakers (each 10 cm above the rat restrainer) to administer the startle stimulus and background white noise (60 dB, 3 – 32 kHz). Noise bursts and background white noise were delivered using a computer-generated sound file that was amplified through an auxiliary amplifier (AUXAMP-B; Kinder Scientific) and was administered to the rats through the two speakers in the sound-attenuated chamber. The Startle Monitor software (Build 06262-18; Kinder Scientific) was used to program the presentation, timing and sequencing of all auditory, tactile and visual stimuli. A control chassis (SM100CC Control Chassis; Kinder Scientific) with an independent microprocessor controller provided a stable interface between the data collection effort and the host personal computer. After each baseline startle testing, fear conditioning training and FPS testing session, rats were returned to their respective home cages in the vivarium. Prior to subsequent testing and/or training sessions, the apparatus was thoroughly cleaned with a soap and water-wetted paper towel, or paper towel with 95% alcohol for FPS startle so as to not interfere with electrical circuits, and the floor bars were cleaned free of dried urine/feces with medium-grit sandpaper to ensure that the current flow was not obstructed.

2.1.2.3. Baseline acoustic startle test for matching: Following six days of acclimation to the colony, on Day −38, (for experimental timeline, see Figure 1) each rat was placed into the animal restrainer inside the sound-attenuated chamber. After 5 min of acclimation to the restrainer, the rat was exposed to the first in a series of 30 acoustic startle (AS+) noise stimuli (10 trials each of 90, 95, and 105 dB noise stimuli) presented quasi-randomly (each intensity only occurred once in a block of 3 noise stimuli) with a 30-sec intertrial interval (ITI). The total session duration was 20 min. After the baseline startle test for matching, the subjects were matched into groups of 12 such that each group had equivalent baseline mean startle amplitudes.

2.1.2.4. Fear conditioning: Starting twenty-four hours after the baseline acoustic startle test for matching, i.e., on days −37 and −36, rats were each placed back into the same animal restrainer/chamber on each of 2 consecutive days (separated by 24 h) for fear conditioning (i.e., training for FPS). Fear conditioning consisted of 5 min of acclimation to the restrainer followed by the presentation of the first of 10 conditioned (CS, light; 115 lux) -

Author Manuscript Author Manuscript Author Manuscript Author Manuscript

unconditioned stimuli (US, footshock) pairings (variable ITI = 4 min; 3-5 min range). The light lasted for 3.7 sec and co-terminated with the footshock (0.6 mA, 0.5 sec). The total session duration was about 45 min.

2.1.2.5. Fear-potentiated startle (FPS) testing: On each of days 1-6, starting 36 d following the final day of two days of fear conditioning, rats were each returned to the same animal restrainer/chamber daily. After 5 min of acclimation to the restrainer, the rats were exposed to the first of 15 noise bursts (CS−/AS+ trials; 5 trials each at 90, 95 and 105 dB; presented quasi-randomly with each intensity only occurring once in a block of 3 trials; ITI = 30 sec), which were called “Leaders”. Thirty seconds after the last “Leader” trial, the rats were exposed to the first of 60 test trials (ITI = 30 sec). Half of the trials involved a 0.5 sec AS+ being administered 3.2 sec after the onset of the light (conditioned stimulus, CS+), which had been previously paired with shock, and co-terminated with the light (CS+/AS+ trials). For the other half of the trials, rats were presented with the AS+ (0.5 sec) in the dark, in the absence of the light (CS−/AS+ trials). There were 60 total trials for each of the CS +/AS+ (30 trials) and CS−/AS+ (30 trials) trials with 9–11 trials at each intensity of 90 (9 – 11 CS−/AS+ and 9 – 11 CS+/AS+), 95 (9 – 11 CS−/AS+ and 9 – 11 CS+/AS+) and 105 dB (9 – 11 CS−/AS+ and 9 – 11 CS+/AS+) noise stimuli and presented quasi-randomly with the restriction that each trial type only occurred once within each successive block of 6 trials. After the 60 trials there were an additional 15 acoustic noise bursts (CS−/AS+ trials; 5 trials each at 90, 95 and 105 dB; presented quasi-randomly with each intensity only occurring once in a block of 3 trials; ITI = 30 sec), which were called “Trailers”. Overall, each session lasted around 50 min. The daily assessment for FPS over the 6-day period served to determine the rate of extinction learning to the CS+. Within-session extinction was determined based on measurement of FPS response during the average of the first block of 90 dB, 95 dB, 105 dB FPS trials (3 CS+/AS+ trials and 3 CS−/AS+ trials per block) after Leaders and the average of the last block of 90 dB, 95 dB, and 105 dB FPS trials (3 CS+/AS + trials and 3 CS−/AS+ trials per block) on each day.

2.2. Euthanasia and brain collection

Rats were euthanized 24 h following the last testing session using an overdose of sodium pentobarbital (Fatal Plus®, Vortech Pharmaceuticals Ltd., Dearborn, MI, USA; 200 mg/kg, i.p.) after which brains were dissected and immediately frozen on dry ice.

2.3. *In situ* hybridization histochemistry

Previously published methods were used for *in situ* hybridization histochemistry (Day and Akil, 1996; Fox et al., 2017; Loupy et al., 2018). Brains were placed into a rat brain matrix and blocked to align with the coronal plane. After blocking brains were sectioned into 12-μm thick sections on a cryostat (Leica CM 1950, Leica Biosystems, Buffalo Grove, IL, USA), and slices were collected beginning approximately at −7.244 mm to −8.504 mm from bregma (Paxinos and Watson, 1998) and placed in a series of 7 sets of sections, thaw-mounted on Histobond® slides (Cat. No. 16,004-406; VWR, West Chester, PA, USA) and stored at −80 °C.

Author Manuscript Author Manuscript Author Manuscript Author Manuscript

2.3.1. Riboprobe preparation—Riboprobes targeting were generated using standard transcription methods, as described previously (Day and Akil, 1996). Riboprobes used in this study were designed to detect: *Tph2* mRNA, encoding the rate-limiting enzyme in the biosynthesis of serotonin; *Htr1a* mRNA, encoding the serotonin receptor subtype 1A; *Slc6a4* mRNA, encoding the high-affinity, low-capacity, sodium-dependent serotonin transporter; *Slc22a3* mRNA, encoding the corticosterone-sensitive, low-affinity, high-capacity, sodium-independent organic cation transporter 3 (OCT3); and *Crhr2* mRNA, encoding the corticotropin-releasing hormone receptor 2.

A sulfur 35 uridine-5'-triphosphate ([[^{35}S]-UTP)-labeled riboprobe was used for detection of *Tph2* mRNA, i.e., a 462 base (1552-2013) antisense riboprobe complementary to the rat cDNA encoding Tph2 (*Tph2*, National Center for Biotechnology Information (NCBI) Reference Sequence: NC_005106.4, from C.A. Lowry (Gardner et al., 2009).

A [^{35}S]-UTP-labeled riboprobe was used for detection of *Htr1a* (from Dr. Stanley J. Watson) mRNA, i.e., a 911 base (333-1243) antisense riboprobe complementary to the rat cDNA encoding Htr1a (i.e., *Htr1a*, NCBI Reference Sequence; NC 005101.4).

A [^{35}S]-UTP-labeled riboprobe was used for detection of *Slc6a4* (originally from Dr. Stanley J. Watson, re-subcloned by H.E.W. Day) mRNA, i.e., a 491 base (828-1318) antisense riboprobe complementary to the rat cDNA encoding Slc6a4 (i.e., *Slc6a4*, NCBI Reference Sequence; NC_005109.4).

A [^{35}S]-UTP-labeled riboprobe was used for detection of *Slc22a3* mRNA, i.e., a 1081 base (1313-2393) antisense riboprobe complementary to the rat cDNA encoding OCT3 (*Slc22a3*, NCBI Reference Sequence: NM_019230.1, designed by M.R. Arnold and H.E.W. Day). Sense and antisense riboprobes were created by adding the T7 phage and clamp sequences (5′-GCGTAATACGACTCACTATAGGGAGA-3′) to the 5′ end of the forward and reverse primer sequence (Eckalbar et al., 2012). The OCT3 forward primer sequence was AGTGCAATGGGAAACACCTCTCG and the reverse primer sequence was TGCCAGGCCTTGATATGTTCATCC.

A [^{35}S]-UTP-labeled riboprobe was used for detection of *Crhr2* mRNA, i.e., using a 464 base (330-793) antisense riboprobe (from Dr. Robert Thompson) complementary to the rat cDNA encoding *Crhr2* (i.e., *crhr2*, NCBI Reference Sequence; NC_005103.4). Riboprobes were radiolabeled via *in vitro* transcription, incorporating [^{35}S]-UTP. Briefly, a nucleotide mix of adenosine triphosphate (ATP), cytidine triphosphate (CTP), guanosine triphosphate (GTP) (1.1 µl of 10 mM each) and uridine-5'-triphosphate (UTP) (1.1 µl of 0.2 mM was added to 2.2 µl 10x transcription buffer (Cat. no. FP021; Promega, Madison, WI, USA), and 0.22 µl 1 M dithiothreitol (DTT). From this solution, 6.2 µl was withdrawn and added to 1 µl (2 µg) cut DNA (antisense or sense), 1.8 µl RNase inhibitor (RNaseOUT, Cat. no. 100000840; Invitrogen, Carlsbad, CA, USA), 4 µl [^{35}S]-UTP (1250 Ci/mmol; Cat. no. NEG039H001MC; New England Nuclear-Perkin Elmer, Boston, MA, USA) and 2 µl of the appropriate RNA polymerase (T3 for antisense and T7 for sense [Cat. no. P208C and P207B, respectively; Promega]). The mixture was incubated at 37 °C for 1 h. The template DNA was then removed by digestion with 0.75 µl RNase-free DNase I (RQ1 DNase Stop

Author Manuscript Author Manuscript Author Manuscript Author Manuscript

Solution, Cat. no. M199A; Promega) for 15 min at 37 °C. The probe was precipitated by ethanol in the presence of 0.5 mg/ml glycogen carrier and redissolved in 100 μl water. Probe activity (1 μl) was counted in a 5-ml volume of scintillation fluid (Ready Safe, Cat. no. p/n484013-ae; Beckman Coulter, Fullerton, CA, USA) with a beta counter (Beckman LS 3801, ser. no. 7013835) and was typically 3–4 X 10^6 counts per minute (cpm).

2.3.2. In situ hybridization histochemistry—Tissue sections were fixed in 4% paraformaldehyde for 1 h, acetylated in 0.1 M triethanolamine hydrochloride with 0.25% acetic anhydride for 10 min, and dehydrated through graded alcohols. Sections were hybridized overnight at 55 °C with a [^{35}S]-UTP-labeled riboprobe diluted in hybridization buffer containing 50% formamide, 10% dextran sulfate, 2× saline sodium citrate (SSC), 50 mM phosphate-buffered saline (PBS), pH 7.4, 1× Denhardt's solution, and 0.1 mg/ml yeast tRNA. The following day, sections were treated with RNase A, 200 μg/ml at 37 °C for 1 h, and washed to a final stringency of 0.1× SSC at 65 °C (1 h). Dehydrated sections were exposed to x-ray film (BioMax MR; Eastman Kodak, Rochester, NY, USA) for region- and probe-appropriate times: *Tph2,* 3 days; *Htr1a*, 14 days; *Slc6a4*, 7 days; *Slc22a3,* 56 days; *Crhr2*, 6 days, prior to film development.

2.3.3. Imaging and densitometry of in situ hybridization histochemistry autoradiograms—Autoradiographic images of probes bound to *Tph2, Htr1a*, *Slc6a4*, *Slc22a3,* and *Crhr2* mRNA, together with ^{14}C-labeled standards, were measured using a computer-assisted image analysis system.

Analysis was performed on a personal computer using the publicly available National Institutes of Health (NIH)-developed image analysis software ImageJ (https://imagej.nih.gov/ij/). All digital images of the x-ray films were taken while blinded to the treatment groups. Virtual matrices in the shape of each subregion of the dorsal raphe nucleus (DR), median raphe nucleus (MnR), pontomesencephalic reticular formation (PMRF), and B9 serotonergic cell group were created, overlaid with the image, and the "mean gray value (GV) x area" within each matrix, taking into account only the area of the above-threshold signal, was measured. During the entire analysis a constant threshold function was applied, which determined the area that was actually measured within each matrix. Thus, all pixels with a gray density below threshold were automatically excluded. The individual background of each image was measured using a control macro just lateral to the medial longitudinal fasciculus (mlf). Each subregion average mean gray value had this background value subtracted.

Rostrocaudal analysis atlases for *Tph2, Htr1a, Slc6a4, Slc22a3*, and *Crhr2* expression in the DR, MnR, PMRF, and B9 serotonergic cell group were created by comparing the image of the tissue sections with a stereotaxic rat brain atlas (Paxinos and Watson, 1998). According to Paxinos and Watson (Paxinos and Watson, 1998), each rostrocaudal level of the DR was further divided into five subregions (Figure 3 (*Tph2*); Figures S5 (*Htr1a*), S8 (*Slc6a4*), S12 (*Slc22a3*), and S16 (*Crhr2*)). The MnR, PMRF, and serotonergic cell group B9 were not further divided. At each rostrocaudal level, the mean gray value x area values for the left and right sides of each dorsal raphe nucleus ventrolateral part/ventrolateral periaqueductal gray (DRVL/VLPAG), PMRF, and B9 serotonergic cell group were averaged and averaged values

Author Manuscript Author Manuscript Author Manuscript Author Manuscript

were used for statistical analyses. Overall mRNA expression within the five subregions of the DR, as well as in the MnR, PMRF, and B9 serotonergic cell group, were displayed by averaging background-corrected mean gray value x area values across all rostrocaudal levels per treatment group. A total of 16 rostrocaudal levels were studied for *Tph2, Htr1a*, and *Slc6a4* mRNA expression, while 12 rostrocaudal levels were studied for *Slc22a3* and *Crhr2* mRNA (Figure 3 (*Tph2*); Figures S5 (*Htr1a*), S8 (*Slc6a4*), S12 (*Slc22a3*), and S16 (*Crhr2*)). The subdivisions studied were summarized into the following subregions and regions: B9, −7.244 mm to −8.000 mm from bregma; dorsal raphe nucleus, caudal part (DRC), −8.336 mm to −8.504 mm from bregma; dorsal raphe nucleus, dorsal part (DRD), −7.244 mm or −7.580 mm to −8.252 mm from bregma; dorsal raphe nucleus, interfascicular part (DRI), −8.252 mm to −8.504 mm from bregma; dorsal raphe nucleus, ventral part (DRV), −7.244 mm or −7.580 mm to −8.504 mm from bregma; DRVL/VLPAG, −7.748 mm to −8.336 mm from bregma; MnR, −7.244 mm or −7.580 mm to −8.504 mm from bregma; PMRF, −7.244 mm to −7.496 mm from bregma.

2.4. Statistical analysis

Statistical analyses were conducted using the software package IBM statistical package for the social sciences (version 24.0, SPSS., Inc Chicago, IL, USA). All tests were two-tailed with a level of significance of 0.05. To account for missing data and individual differences, we used a linear mixed model (LMM) approach, which has been recommended for analysis of repeated measures (Judd et al., 2012). Extreme statistical outliers were identified using Grubbs' test for single outliers using two-sided $\alpha = 0.05$ (Grubbs, 1969) and were removed from the analysis. A survey of LMMs with different covariance structures was performed and the model with the best −2 log-likelihood value, an information criterion function used for goodness of fit, was selected (i.e., the covariance structure with the lowest −2 log-likelihood value was used). For analysis of FPS data, *M. vaccae* and day were used as fixed effects. Post hoc between-subjects comparisons were made using Fisher's least significant difference (LSD) test and post hoc within-subjects comparisons were made using paired *t*-tests. For analysis of *in situ* hybridization histochemistry data, we used a random intercept and slope model, modeling mRNA expression (mean background-corrected gray values x area) for each rostrocaudal level within subregions of the DR, MnR, PMRF, as well as B9 serotonergic cell group. Sixteen covariate structures were assessed, including: diagonal; compound symmetry; correlation compound symmetry; heterogeneous compound symmetry; Huynh-Feldt; first-order ante-dependence; first-order autoregressive; heterogeneous first-order autoregressive; first-order analytic (constant diagonal offset); first-order analytic (heterogeneous diagonal offset); identity; toeplitz; heterogeneous toeplitz; ARMA (1,1); unstructured; and unstructured correlations. The level-one model is as follows:

$$\begin{aligned} &mean\ background-corrected\ gray\ values\ x\ area_{ij} \\ &\quad = \beta_0 + \beta_1 Treatment_i + \beta_2 Rostrocaudal\ level_j + \beta_3 Raphe\ subregion_k \\ &\quad + \beta_4 (Treatment * Raphe\ subregion)_{ik} \\ &\quad + \beta_5 (Rostrocaudal\ level\ (Raphe\ subregion))_{jk} \\ &\quad + \beta_6 (Treatment * Rostrocaudal\ level\ (Raphe\ subregion))_{ijk} \\ &\quad + Covariates_m + \varepsilon_{ijk} \end{aligned}$$

Author Manuscript Author Manuscript Author Manuscript Author Manuscript

Random intercepts and slopes for the covariates were modeled on each individual participant. The individual β values in the above equation explain the partial effects of *M. vaccae* treatment (β_1 either *M. vaccae* or BBS vehicle), rostrocaudal level (β_2, 84 μm-thick coronal slices) raphe subregion (β_3, DRD, DRV, DRVL/VLPAG, DRC, DRI, PMRF, B9 serotonergic cell group, MnR) and the interaction of treatment, rostrocaudal level and subregion of the DR.

Results

Effects of M. vaccae on between-session fear extinction

Linear mixed model analysis of between-session fear extinction revealed a main effect of *M. vaccae* ($F_{(1,19.6)} = 9.1$; $p < 0.01$) and a main effect of extinction training day ($F_{(6,20.3)} = 5.0$; $p < 0.01$) (Figure 2A). Post hoc analysis of between-session fear extinction revealed that there were no differences in FPS between *M. vaccae*- and vehicle-immunized controls on day 1 of fear extinction training (Figure 2A). In contrast, *M. vaccae*-immunized rats showed decreased FPS, relative to vehicle-treated controls, on days 2 ($p < 0.001$) and 3 ($p < 0.007$) of fear extinction. Among rats treated with *M. vaccae*, paired *t*-tests revealed a difference between extinction day 1 and the following extinction days: extinction day 3 ($t_{(10)} = 2,70$, $p < 0.022$); extinction day 4 ($t_{(10)} = 2.41$, $p < 0.037$); extinction day 5 ($t_{(11)} = 2.90$, $p < 0.014$); extinction day 6 ($t_{(11)} = 2.85$, $p < 0.016$); and spontaneous recovery on day 20 ($t_{(11)} = 3.79$, $p < 0.003$; Figure 2A). In comparison, among vehicle-treated rats, paired *t*-tests revealed a difference in FPS between extinction day 1 and extinction day 6 ($t_{(11)} = 2.98$, $p < 0.012$; Figure 2A).

Effects of M. vaccae on within-session fear extinction

Linear mixed model analysis of within-session extinction of FPS across days 1– 6 and spontaneous recovery on day 20 revealed an *M. vaccae* x trial block within day interaction ($F_{(54,219)} = 1.68$, $p < 0.005$). On day 1, the first day of fear extinction training, paired *t*-tests revealed within-session extinction in *M. vaccae*-treated rats ($t_{(10)} = 3.04$, $p < 0.012$; Figure 2B) but not vehicle-treated rats. On days 2 ($p < 0.05$) and 3 ($p < 0.05$) *M. vaccae*-immunized animals had a lower FPS compared to vehicle-treated rats at the beginning of the extinction testing session. Vehicle-treated rats showed within-session extinction on day 2 ($t_{(10)} = 2.30$, $p < 0.05$) and day 3 ($t_{(10)} = 2.74$, $p < 0.05$; Figure 2B).

In situ hybridization histochemistry

In situ hybridization histochemistry was used to evaluate the effects of *M. vaccae* immunization on expression of a panel of genes thought to be important for control of serotonergic neurotransmission, including *Tph2, Htr1a*, *Slc6a4, Slc22a3,* and *Crhr2.*

Tph2 mRNA expression

Analysis of *Tph2* mRNA expression using the overall LMM revealed an *M. vaccae* by rostrocaudal level interaction ($F_{(15,127.8)} = 2.6$; $p < 0.01$; Figure 3A-P; Figure 4A-B; Supplemental Figure 1A-H; Supplemental Figure 1A-H; Supplemental Table 1). When *Tph2* mRNA expression was averaged at each rostrocaudal level throughout the extent of the DR, MnR, B9 supralemniscal serotonergic cell group, and PMRF, *M. vaccae* increased *Tph2*

Author Manuscript Author Manuscript Author Manuscript Author Manuscript

mRNA at rostrocaudal level −8.000 mm from bregma (Figure 4A; $p < 0.05$). There were no effects of *M. vaccae* on *Tph2* mRNA expression within individual subregions of the DR, MnR, B9, or PMRF when *Tph2* mRNA expression was averaged across all rostrocaudal levels of each subregion (Supplemental Figure 2A-H) or on overall *Tph2* mRNA expression across all rostrocaudal levels of all subregions studied (Figure 4B).

Htr1a mRNA expression

Analysis of *Htr1a* mRNA expression using the overall LMM revealed an *M. vaccae* by rostrocaudal level interaction ($F_{(15,134.3)} = 3.9$; $p < 0.001$; Supplemental Figure 3A-P Supplemental Figure 5A-H; Supplemental Table 2). Secondary LMMs were used to determine effects of treatment within each subregion of the DR, MnR, PMRF, and B9 serotonergic cell group. When *Htr1a* mRNA expression was averaged at each rostrocaudal level throughout the rostrocaudal extent of the DR, MnR, B9 supralemniscal serotonergic cell group, and PMRF, *M. vaccae* decreased *Htr1a* mRNA expression at rostrocaudal level −8.000 mm from bregma (***$p < 0.001$; Supplemental Figure 4A). Linear mixed model analysis of specific subregions revealed an *M. vaccae* x rostrocaudal level interaction in the DRD ($F_{(12,30.8)} = 2.2$, $p < 0.05$) (Supplemental Figure 5A). Specifically, *M. vaccae* decreased *Htr1a* mRNA expression at −8.000 mm from bregma in the DRD ($p < 0.05$; Supplemental Figure 5A). *M. vaccae* also increased the mean *Htr1a* mRNA expression within the MnR (Supplemental Figure 6F).

Slc6a4 mRNA expression

Analysis of *Slc6a4* mRNA expression using the overall LMM revealed an *M. vaccae* by rostrocaudal level interaction ($F_{(15,149.0)} = 2.1$; $p < 0.015$; Supplemental Figure 7A-P; ; Supplemental Figure 9A-H; Supplemental Table 3). Secondary LMM were used to determine effects of treatment within each subregion of the DR, MnR, PMRF, and B9 serotonergic cell group. Linear mixed model analysis of specific subregions revealed an *M. vaccae* x rostrocaudal level interaction in the B9 serotonergic cell group ($F_{(11,42.3)} = 2.3$, $p < 0.05$; Supplemental Figure 9G, Supplemental Table 3). *M. vaccae* decreased *Slc6a4* mRNA at −8.168 mm ($p < 0.05$) and – 8.252 mm ($p < 0.01$) from bregma (Supplemental Figure 9G). Additionally, *M. vaccae* increased overall mean *Slc6a4* mRNA expression across all regions studied ($t_{(1385)} = 2.26$, $p < 0.05$; Supplemental Figure 8B).

Slc22a3 mRNA expression

Analysis of *Slc22a3* mRNA expression using the overall LMM revealed no effects of *M. vaccae* or interactions among *M. vaccae,* raphe subregion, or rostrocaudal level within the DR or MnR (Supplemental Figure 11A-L; Supplemental Figure 12A-B; Supplemental Figure 13A-F; Supplemental Figure 14A-F; Supplemental Table 4).

Crhr2 mRNA expression

Analysis of *Crhr2* mRNA expression using the overall LMM revealed no effects of *M. vaccae* or interactions among *M. vaccae,* raphe subregion, or rostrocaudal level within the DR or MnR (Supplemental Figure 15A-L; Supplemental Figure 16A-B;Supplemental Figure 17A-G; Supplemental Figure 18A-G; ; Supplemental Table 5).

Author Manuscript Author Manuscript Author Manuscript Author Manuscript

Discussion

Treatment with a heat-killed preparation of *M. vaccae* NCTC 11659, with three weekly immunizations initiated 24 h after fear conditioning, enhanced both between-session and within-session fear extinction in a rat FPS paradigm. Immunization with *M. vaccae* had no effect on the acquisition of FPS; i.e., the *M. vaccae*-immunized and vehicle-immunized rats showed the same level of FPS on the first day of fear extinction training, assessed 36 days after fear conditioning. However, *M. vaccae*-immunized rats had enhanced between-session fear extinction, with lower FPS compared to vehicle-immunized controls on days 2 and 3 of fear extinction training. Furthermore, within-subject comparisons revealed reduced FPS in *M. vaccae*-immunized rats by day 3 of fear extinction training; in contrast, vehicle-immunized rats did not show reductions in FPS until day 6 of fear extinction training. *M. vaccae*-immunized rats also showed enhanced within-session fear extinction relative to vehicle-immunized controls on day 1 of fear extinction training. When assessed 41 days after the final immunization (i.e., 15 days after the final day of extinction training), *M. vaccae* had no consistent effects on expression of serotonergic genes (*Tph2, Htr1a, Slc6a4, Slc22a3*), or genes that control serotonergic signaling (*Crhr2*), within the brainstem dorsal and median raphe nuclei.

Immunization with *M. vaccae* had no effect on the acquisition of FPS, i.e., the *M. vaccae*-immunized and vehicle-immunized rats showed the same level of FPS on the first day of fear extinction training. The findings in the current study are consistent with previous studies in which immunizations with *M. vaccae* prior to fear conditioning had no effect on either acoustic startle or fear acquisition in the FPS paradigm, but instead enhanced between-session and within-session fear extinction (Fox et al., 2017; Loupy et al., 2018).

Treatment with a heat-killed preparation of *M. vaccae* NCTC 11659 with immunizations initiated 24 h after fear conditioning enhanced both between-session and within-session fear extinction in the rat FPS paradigm, effects that may be dependent on enhanced immunoregulation. The effects of *M. vaccae* to enhance fear extinction were long-lasting (i.e., 21 [current study] to 25 days between the final *M. vaccae* immunization and fear-extinction training (Fox et al., 2017; Loupy et al., 2018)). Similar long-lasting effects of *M. vaccae* were observed on anxiety-like defensive behavioral responses in a chronic subordinate colony housing (CSC) model in mice (Reber et al., 2016b). The protective effects of *M. vaccae* on anxiety-like behaviors in the CSC model were absent following depletion of Treg, suggesting that the stress-protective effects are dependent on Treg (Reber et al., 2016b). These findings parallel previous findings that immunization with the same strain of *M. vaccae* prevents allergic airway inflammation in a murine model of asthma in a Treg-dependent manner (Zuany-Amorim et al., 2002). The protective effects of *M. vaccae* in allergic airway inflammation have also been demonstrated to be dependent on the production of anti-inflammatory cytokines, including interleukin (IL) 10 and transforming growth factor beta (Zuany-Amorim et al., 2002). The half-life of newly differentiated Treg is estimated to be 27 days in C57BL/6 mice (Depis et al., 2016). Therefore, induction of Treg is a reasonable hypothesis to explain the long-lasting stress-protective and anti-inflammatory effects observed in diverse model systems. An alternative, but not mutually exclusive, hypothesis is that *M. vaccae* induces long-lasting anti-inflammatory responses in the central

Author Manuscript Author Manuscript Author Manuscript Author Manuscript

nervous system (Fonken et al., 2018; Frank et al., 2018a). As a final alternative, we recently characterized a novel triacylglycerol that seems to be unique to mycobacteria, 1,2,3-tri [*Z*-10-hexadecenoyl] glycerol, the free fatty acid form of which, 10(*Z*)-hexadecenoic acid, acts as a ligand at host peroxisome proliferator-activated receptor alpha (PPARα)(Smith et al., 2019). Recent studies have demonstrated that the endocannabinoid, palmitoylethanolamide (PEA), also acts as an agonist at PPARα (Guida et al., 2017; Lo Verme et al., 2005). PEA increases the biosynthesis of allopregnanolone, an endocannabinoid, in the hippocampus and amygdala, effects that are associated with faster fear extinction learning in mice (Locci and Pinna, 2017; Pinna 2018; Sasso et al., 2012)). Future studies should determine if lipid constituents of *M. vaccae*, i.e., 1,2,3-tri [*Z*-10-hexadecenoyl] glycerol or 10(*Z*)-hexadecenoic acid, are sufficient to induce the enhanced fear extinction learning demonstrated using whole, heat-killed *M. vaccae*, and to what extent these effects are mediated by PPARα.

When assessed 41 days after the final immunization, *M. vaccae* had no consistent effects on expression of serotonergic genes, or genes that control serotonergic signaling, within the brainstem dorsal and median raphe nuclei. In a previous study, *M. vaccae* immunization prior to fear conditioning, as opposed to after fear conditioning, as done here, altered serotonergic gene expression. For example, immunization with *M. vaccae* prior to fear conditioning decreased *Tph2* mRNA expression, encoding tryptophan hydroxylase 2, the rate-limiting enzyme for serotonin synthesis, within the MnR and decreased *Slc22a3* mRNA expression (which encodes organic cation transporter 3, a corticosterone-sensitive, low-affinity, high-capacity monoamine transporter), within the DRD and DRV. However, the timelines between the final *M. vaccae* immunization and tissue collection were different in the two studies, i.e., 31 days in Fox et al. (2017) versus 41 days in this study. Also of potential relevance, mRNA expression was assessed 24 h following the final day of fear extinction testing in Fox et al. (2017), and, due to testing for spontaneous recovery 14 days following the final day of fear extinction training, mRNA expression was assessed 15 days following the final day of fear extinction testing in the current study. Nevertheless, studies suggest that immunoregulation is an important determinant of brain serotonergic signaling as depletion of Treg decreases hippocampal concentrations of serotonin and the serotonin metabolite, 5-hydroxyindoleacetic acid (5-HIAA) (Kim et al., 2012). Serotonergic projections from the MnR to the hippocampus have been suggested to comprise a stress resilience circuit, as proposed by Deakin and Graeff (Deakin and Graeff, 1991; Paul and Lowry, 2013). Indeed, lesions or pharmacological inhibition of the MnR interfere with contextual fear conditioning, but leave cued fear conditioning intact, supporting a functional connection between the MnR and hippocampal-dependent learning processes (Silva et al., 2004). Reber et al. (2016) found that immunization with *M. vaccae* increased *Tph2* mRNA expression within the rostral portion of the DRD when measured 48 hrs after the last day of CSC stress (Reber et al., 2016b). Future studies are required to determine the time course of the effects of immunizations of *M. vaccae,* or other immunoregulatory and anti-inflammatory interventions, on serotonergic signaling.

Author Manuscript Author Manuscript Author Manuscript Author Manuscript

Conclusions and future directions

The studies described here show that immunization with *M. vaccae* following fear conditioning, as opposed to before fear conditioning, as shown in previous studies (Fox et al., 2017; Loupy et al., 2018), is able to enhance both between-session and within-session fear extinction. These studies are consistent with previous studies showing that stress-induced enhancement of the acoustic startle reflex was attenuated in RAG2$^{-/-}$ mice, suggesting a role for peripheral mature T cells in modulating stress-induced enhancement of anxiety- and fear-like defensive behavioral responses (Clark et al., 2014; Clark et al., 2016). These findings suggest that immunization with *M. vaccae*, or other immunoregulatory approaches, might be considered as novel therapeutic approaches to treatment of anxiety disorders, or trauma- and stressor-related disorders, such as PTSD. Persons with a diagnosis of PTSD have been shown to have enhanced FPS (Morgan et al., 1995) as well as fear extinction resistance in a number of paradigms (Norrholm et al., 2011), suggesting a need for translational studies. Individuals with a diagnosis of PTSD have also been found to have increased secretion of proinflammatory cytokines, including IL-1β, IL-6, and TNF, from peripheral blood mononuclear cells prior to and after LPS stimulation (Gola et al., 2013). Furthermore, neuroinflammatory genes have been associated with individuals diagnosed with PTSD and comorbid conditions (Zass et al., 2017). The current study utilized a cue, light, in the FPS paradigm and future studies would benefit from exploring the effects of immunization with *M. vaccae* in traditional contextual and cued-fear conditioning paradigms. Future studies of the effects of immunization with *M. vaccae* on stress-induced enhancement of fear acquisition, or stress-induced enhancement of resistance to fear extinction are needed to further validate potential use of *M. vaccae* or other immunoregulatory approaches in the prevention and treatment of trauma- and stressor-related disorders including PTSD.

Supplementary Material

Refer to Web version on PubMed Central for supplementary material.

Acknowledgements

We gratefully acknowledge Zachary D. Barger for proofreading the article. Funding: This work was supported by the National Institute of Mental Health (grant number 1R21MH116263). Dr. Christopher A. Lowry is supported by the National Institute of Mental Health (grant number 1R21MH116263), Department of the Navy, Office of Naval Research Multidisciplinary University Research Initiative (MURI) Award (grant number N00014-15-1-2809), Department of Veterans Affairs Office of Research and Development (VA-ORD) RR&D Small Projects in Rehabilitation Research (SPiRE) (I21) (grant number 1 I21 RX002232-01), Colorado Clinical & Translational Sciences Institute (CCTSI) Center for Neuroscience (grant number CNSTT-15-145), the Colorado Department of Public Health and Environment (CDPHE; grant number DCEED-3510), and the Alfred P. Sloan Foundation (grant number, G-2016-7077). Christopher A. Lowry serves on the Scientific Advisory Board of Immodulon Therapeutics Ltd.

List of Abbreviations

A/N	analog to digital
AS−	acoustic startle absent

Author Manuscript Author Manuscript Author Manuscript Author Manuscript

AS+	acoustic startle present
ATP	adenosine triphosphate
B9	B9 serotonergic cell group
BBS	borate-buffered saline
CAPS	Clinician administered PTSD score
cpm	counts per minute
Crhr2	corticotropin-releasing hormone receptor 2
CS	conditioned stimulus
CS−	conditioned stimulus absent
CS+	conditioned stimulus present
CTP	cytidine triphosphate
DR	dorsal raphe nucleus
DRD	dorsal raphe nucleus, dorsal part
DRI	dorsal raphe nucleus, interfasicular part
DRV	dorsal raphe nucleus, ventral part
DRVL	dorsal raphe nucleus, ventrolateral part
DTT	dithiothreitol
FPS	fear-potentiated startle
GV	gray value
GTP	guanosine triphosphate
Htr1a	serotonin receptor subtype 1A
i.p.,	intraperitoneal
ITI	intertrial interval
LSD	least significant difference
LMM	linear mixed model
MnR	median raphe nucleus
Mv	*Mycobacterium vaccae* NCTC 11659
N	Newtons
NCBI	National Center for Biotechnology Information

Author Manuscript Author Manuscript Author Manuscript Author Manuscript

NCTC	National Collection of Type Cultures
NIH	National Institutes of Health
PBS	phosphate-buffered saline
PMRF	pontomesencephalic reticular formation
SSC	saline sodium citrate
s.c.	subcutaneous
Slc6a4	solute carrier family 6 member 4
Slc22a3	solute carrier family 22 member 3
Tph2	tryptophan hydroxylase 2
UTP	uridine-5'-triphosphate
US	unconditioned stimulus
Veh	vehicle
VLPAG	ventrolateral periaqueductal gray

References

Bocchio M, McHugh SB, Bannerman DM, Sharp T, Capogna M, 2016 Serotonin, amygdala and fear: assembling the puzzle. Front Neural Circuits 10, 24. [PubMed: 27092057]

Clark SM, Sand J, Francis TC, Nagaraju A, Michael KC, Keegan AD, Kusnecov A, Gould TD, Tonelli LH, 2014 Immune status influences fear and anxiety responses in mice after acute stress exposure. Brain Behav Immun 38, 192–201. [PubMed: 24524915]

Clark SM, Soroka JA, Song C, Li X, Tonelli LH, 2016 CD4(+) T cells confer anxiolytic and antidepressant-like effects, but enhance fear memory processes in Rag2(−/−) mice. Stress 19, 303–311. [PubMed: 27295202]

Davis M, 1986 Pharmacological and anatomical analysis of fear conditioning using the fear-potentiated startle paradigm. Behav Neurosci 100, 814–824. [PubMed: 3545257]

Davis M, Astrachan DI, 1978 Conditioned fear and startle magnitude: effects of different footshock or backshock intensities used in training. J Exp Psychol Anim Behav Process 4, 95–103. [PubMed: 670892]

Davis M, Falls WA, Campeau S, Kim M, 1993 Fear-potentiated startle: a neural and pharmacological analysis. Behav Brain Res 58, 175–198. [PubMed: 8136044]

Day HE, Akil H, 1996 Differential pattern of *c-fos* mRNA in rat brain following central and systemic administration of interleukin-1-beta: implications for mechanism of action. Neuroendocrinology 63, 207–218. [PubMed: 8677009]

Deakin JF, Graeff FG, 1991 5-HT and mechanisms of defence. J Psychopharmacol 5, 305–315. [PubMed: 22282829]

Depis F, Kwon HK, Mathis D, Benoist C, 2016 Unstable FoxP3+ T regulatory cells in NZW mice. Proc Natl Acad Sci U S A 113, 1345–1350. [PubMed: 26768846]

Eckalbar WL, Lasku E, Infante CR, Elsey RM, Markov GJ, Allen AN, Corneveaux JJ, Losos JB, DeNardo DF, Huentelman MJ, Wilson-Rawls J, Rawls A, Kusumi K, 2012 Somitogenesis in the anole lizard and alligator reveals evolutionary convergence and divergence in the amniote segmentation clock. Dev Biol 363, 308–319. [PubMed: 22178152]

Author Manuscript Author Manuscript Author Manuscript Author Manuscript

Falls WA, Miserendino MJ, Davis M, 1992 Extinction of fear-potentiated startle: blockade by infusion of an NMDA antagonist into the amygdala. J Neurosci 12, 854–863. [PubMed: 1347562]

Fonken LK, Frank MG, D'Angelo HM, Heinze JD, Watkins LR, Lowry CA, Maier SF, 2018 *Mycobacterium vaccae* immunization protects aged rats from surgery-elicited neuroinflammation and cognitive dysfunction. Neurobiol Aging 71, 105–114. [PubMed: 30118926]

Fox JH, Hassell JE Jr., Siebler PH, Arnold MR, Lamb AK, Smith DG, Day HEW, Smith TM, Simmerman EM, Outzen AA, Holmes KS, Brazell CJ, Lowry CA, 2017 Preimmunization with a heat-killed preparation of *Mycobacterium vaccae* enhances fear extinction in the fear-potentiated startle paradigm. Brain Behav Immun 66, 70–84. [PubMed: 28888667]

Frank MG, Fonken LK, Dolzani SD, Annis JL, Siebler PH, Schmidt D, Watkins LR, Maier SF, Lowry CA, 2018a Immunization with *Mycobacterium vaccae* induces an anti-inflammatory milieu in the CNS: Attenuation of stress-induced microglial priming, alarmins and anxiety-like behavior. Brain Behav Immun 73, 352–363. [PubMed: 29807129]

Frank MG, Fonken LK, Watkins LR, Maier SF, Lowry CA, 2018b Could probiotics be used to mitigate neuroinflammation? ACS Chem Neurosci 10, 13–15. [PubMed: 30109920]

Gardner KL, Hale MW, Oldfield S, Lightman SL, Plotsky PM, Lowry CA, 2009 Adverse experience during early life and adulthood interact to elevate *tph2* mRNA expression in serotonergic neurons within the dorsal raphe nucleus. Neuroscience 163, 991–1001. [PubMed: 19647049]

Goenjian AK, Bailey JN, Walling DP, Steinberg AM, Schmidt D, Dandekar U, Noble EP, 2012 Association of TPH1, TPH2, and 5HTTLPR with PTSD and depressive symptoms. J Affect Disord 140, 244–252. [PubMed: 22483952]

Goenjian AK, Noble EP, Steinberg AM, Walling DP, Stepanyan ST, Dandekar S, Bailey JN, 2015 Association of *COMT* and *TPH-2* genes with DSM-5 based PTSD symptoms. J Affect Disord 172, 472–478. [PubMed: 25451452]

Gola H, Engler H, Sommershof A, Adenauer H, Kolassa S, Schedlowski M, Groettrup M, Elbert T, Kolassa IT, 2013 Posttraumatic stress disorder is associated with an enhanced spontaneous production of pro-inflammatory cytokines by peripheral blood mononuclear cells. BMC Psychiatry 13, 40. [PubMed: 23360282]

Grubbs FE, 1969 Procedures for detecting outlying observations in samples. Technometrics 11, 1–21.

Guida F, Luongo L, Boccella S, Giordano ME, Romano R, Bellini G, Manzo I, Furiano A, Rizzo A, Imperatore R, Iannotti FA, D'Aniello E, Piscitelli F, Sca Rossi F, Cristino L, Di Marzo V, de Novellis V, Maione S, 2017 Palmitoylethanolamide induces microglia changes associated with increased migration and phagocytic activity: involvement of the CB2 receptor. Sci Rep 7, 375. [PubMed: 28336953]

Guo M, Liu T, Guo JC, Jiang XL, Chen F, Gao YS, 2012 Study on serum cytokine levels in posttraumatic stress disorder patients. Asian Pac J Trop Med 5, 323–325. [PubMed: 22449527]

Hassell JE Jr., Nguyen KT, Gates CA, Lowry CA, 2018 The impact of stressor exposure and glucocorticoids on anxiety and fear. Curr Top Behav Neurosci. 2018 10 25. doi: 10.1007/7854_2018_63. [Epub ahead of print], 1–51.

Hodes GE, Pfau ML, Leboeuf M, Golden SA, Christoffel DJ, Bregman D, Rebusi N, Heshmati M, Aleyasin H, Warren BL, Lebonte B, Horn S, Lapidus KA, Stelzhammer V, Wong EH, Bahn S, Krishnan V, Bolaños-Guzman CA, Murrough JW, Merad M, Russo SJ, 2014 Individual differences in the peripheral immune system promote resilience versus susceptibility to social stress. Proc Natl Acad Sci U S A 111, 16136–16141. [PubMed: 25331895]

Ipser JC, Stein DJ, 2012 Evidence-based pharmacotherapy of post-traumatic stress disorder (PTSD). Int J Neuropsychopharmacol 15, 825–840. [PubMed: 21798109]

Johnson PL, Molosh A, Fitz SD, Arendt D, Deehan GA, Federici LM, Bernabe C, Engleman EA, Rodd ZA, Lowry CA, Shekhar A, 2015 Pharmacological depletion of serotonin in the basolateral amygdala complex reduces anxiety and disrupts fear conditioning. Pharmacol Biochem Behav 138, 174–179. [PubMed: 26476009]

Jovanovic T, Norrholm SD, Blanding NQ, Davis M, Duncan E, Bradley B, Ressler KJ, 2010 Impaired fear inhibition is a biomarker of PTSD but not depression. Depress Anxiety 27, 244–251. [PubMed: 20143428]

Author Manuscript Author Manuscript Author Manuscript Author Manuscript

Jovanovic T, Norrholm SD, Fennell JE, Keyes M, Fiallos AM, Myers KM, Davis M, Duncan EJ, 2009 Posttraumatic stress disorder may be associated with impaired fear inhibition: relation to symptom severity. Psychiatry Res 167, 151–160. [PubMed: 19345420]

Judd CM, Westfall J, Kenny DA, 2012 Treating stimuli as a random factor in social psychology: A new and comprehensive solution to a pervasive but largely ignored problem. J Pers Soc Psychol 103, 54–69. [PubMed: 22612667]

Kilpatrick DG, Resnick HS, Milanak ME, Miller MW, Keyes KM, Friedman MJ, 2013 National estimates of exposure to traumatic events and PTSD prevalence using DSM-IV and DSM-5 criteria. J Trauma Stress 26, 537–547. [PubMed: 24151000]

Kim SJ, Lee H, Lee G, Oh SJ, Shin MK, Shim T, Bae H, 2012 CD4+CD25+ regulatory T cell depletion modulates anxiety and depression-like behaviors in mice. PLoS One 7, e42054. [PubMed: 22860054]

Langgartner D, Lowry CA, Reber SO, 2019 Old Friends, immunoregulation, and stress resilience. Pflugers Arch 471, 237–269. [PubMed: 30386921]

Lindqvist D, Dhabhar FS, Mellon SH, Yehuda R, Grenon SM, Flory JD, Bierer LM, Abu-Amara D, Coy M, Makotkine T, Reus VI, Bersani FS, Marmar CR, Wolkowitz OM, 2017a Increased pro-inflammatory milieu in combat related PTSD - A new cohort replication study. Brain Behav Immun 59, 260–264. [PubMed: 27638184]

Lindqvist D, Mellon SH, Dhabhar FS, Yehuda R, Grenon SM, Flory JD, Bierer LM, Abu-Amara D, Coy M, Makotkine T, Reus VI, Aschbacher K, Bersani FS, Marmar CR, Wolkowitz OM, 2017b Increased circulating blood cell counts in combat-related PTSD: Associations with inflammation and PTSD severity. Psychiatry Res 258, 330–336. [PubMed: 28942957]

Lindqvist D, Wolkowitz OM, Mellon S, Yehuda R, Flory JD, Henn-Haase C, Bierer M, Abu-Amara D, Coy M, Neylan TC, Makotkine T, Reus VI, Yan X, Taylor NM, Marmar CR, Dhabhar FS, 2014 Proinflammatory milieu in combat-related PTSD is independent of depression and early life stress. Brain Behav Immun 42, 81–88. [PubMed: 24929195]

Lo Verme J, Fu J, Astarita G, La Rana G, Russo R, Calignano A, Piomelli D, 2005 The nuclear receptor peroxisome proliferator-activated receptor-α mediates the anti-inflammatory actions of palmitoylethanolamide. Mol Pharmacol 67, 15–19 [PubMed: 15465922]

Locci A, Pinna G, 2017 Stimulation of the endocannabinoid system by PEA engages neurosteroid biosynthesis to improve anxiety and fear in a PTSD mouse model. Soc. Neurosci. Abstr.

Loupy KM, Arnold MR, Hassell JE Jr., Lieb MW, Milton LN, Cler KE, Fox JH, Siebler PH, Schmidt D, Noronha S, Day HEW, Lowry CA, 2018 Evidence that preimmunization with a heat-killed preparation of *Mycobacterium vaccae* reduces corticotropin-releasing hormone mRNA expression in the extended amygdala in a fear-potentiated startle paradigm. Brain Behav Immun. 2018 12 28. pii: S0889–1591(18)31248-0. doi: 10.1016/j.bbi.2018.12.015. [Epub ahead of print]

Lowry CA, Hollis JH, de Vries A, Pan B, Brunet LR, Hunt JR, Paton JF, van Kampen E, Knight DM, Evans AK, Rook GA, Lightman SL, 2007 Identification of an immune-responsive mesolimbocortical serotonergic system: potential role in regulation of emotional behavior. Neuroscience 146, 756–772. [PubMed: 17367941]

Michopoulos V, Powers A, Gillespie CF, Ressler KJ, Jovanovic T, 2017 Inflammation in fear- and anxiety-based disorders: PTSD, GAD, and beyond. Neuropsychopharmacology 42, 254–270. [PubMed: 27510423]

Milad MR, Pitman RK, Ellis CB, Gold AL, Shin LM, Lasko NB, Zeidan MA, Handwerger K, Orr SP, Rauch SL, 2009 Neurobiological basis of failure to recall extinction memory in posttraumatic stress disorder. Biol Psychiatry 66, 1075–1082. [PubMed: 19748076]

Morath J, Gola H, Sommershof A, Hamuni G, Kolassa S, Catani C, Adenauer H, Ruf-Leuschner M, Schauer M, Elbert T, Groettrup M, Kolassa IT, 2014 The effect of trauma-focused therapy on the altered T cell distribution in individuals with PTSD: evidence from a randomized controlled trial. J Psychiatr Res 54, 1–10. [PubMed: 24726027]

Morgan CA 3rd, Grillon C, Southwick SM, Davis M, Charney DS, 1995 Fear-potentiated startle in posttraumatic stress disorder. Biol Psychiatry 38, 378–385. [PubMed: 8547457]

Myers KM, Carlezon WA Jr., Davis M, 2011 Glutamate receptors in extinction and extinction-based therapies for psychiatric illness. Neuropsychopharmacology 36, 274–293. [PubMed: 20631689]

Author Manuscript Author Manuscript Author Manuscript Author Manuscript

Norrholm SD, Jovanovic T, Olin IW, Sands LA, Karapanou I, Bradley B, Ressler KJ, 2011 Fear extinction in traumatized civilians with posttraumatic stress disorder: relation to symptom severity. Biol Psychiatry 69, 556–563. [PubMed: 21035787]

O'Brien ME, Anderson H, Kaukel E, O'Byrne K, Pawlicki M, Von Pawel J, Reck M, Group S-O-S, 2004 SRL 172 (killed *Mycobacterium vaccae*) in addition to standard chemotherapy improves quality of life without affecting survival, in patients with advanced nonsmall-cell lung cancer: phase III results. Ann Oncol 15, 906–914. [PubMed: 15151947]

Paul ED, Lowry CA, 2013 Functional topography of serotonergic systems supports the Deakin/Graeff hypothesis of anxiety and affective disorders. J Psychopharmacol 27, 1090–1106. [PubMed: 23704363]

Paxinos G, Watson C, 1998 The Rat Brain in Stereotaxic Coordinates. Academic Press, San Diego.

Pinna G, 2018 Biomarkers for PTSD at the Interface of the Endocannabinoid and Neurosteroid Axis. Front Neurosci 12, 482. [PubMed: 30131663]

Reber SO, Langgartner D, Foertsch S, Postolache TT, Brenner LA, Guendel H, Lowry CA, 2016a Chronic subordinate colony housing paradigm: A mouse model for mechanisms of PTSD vulnerability, targeted prevention, and treatment-2016 Curt Richter Award Paper. Psychoneuroendocrinology 74, 221–230. [PubMed: 27676359]

Reber SO, Siebler PH, Donner NC, Morton JT, Smith DG, Kopelman JM, Lowe KR, Wheeler KJ, Fox JH, Hassell JE Jr., Greenwood BN, Jansch C, Lechner A, Schmidt D, Uschold-Schmidt N, Füchsl AM, Langgartner D, Walker FR, Hale MW, Lopez Perez G, Van Treuren W, González A, Halweg-Edwards AL, Fleshner M, Raison CL, Rook GA, Peddada SD, Knight R, Lowry CA, 2016b Immunization with a heat-killed preparation of the environmental bacterium *Mycobacterium vaccae* promotes stress resilience in mice. Proc Natl Acad Sci U S A 113, E3130–3139. [PubMed: 27185913]

Ren J, Friedmann D, Xiong J, Liu CD, Ferguson BR, Weerakkody T, DeLoach KE, Ran C, Pun A, Sun Y, Weissbourd B, Neve RL, Huguenard J, Horowitz MA, Luo L, 2018 Anatomically defined and functionally distinct dorsal raphe serotonin sub-systems. Cell 175, 472–487 e420. [PubMed: 30146164]

Rescorla RA, 2004 Spontaneous recovery. Learn Mem 11, 501–509. [PubMed: 15466300]

Sasso O, Russo R, Vitiello S, Raso GM, D'Agostino G, Iacono A, Rana GL, Vallee M, Cuzzocrea S, Piazza PV, Meli R, Calignano A, 2012 Implication of allopregnanolone in the antinociceptive effect of N-palmitoylethanolamide in acute or persistent pain. Pain 153, 33–41. [PubMed: 21890273]

Siebler PH, Heinze JD, Kienzle DM, Hale MW, Lukkes JL, Donner NC, Kopelman JM, Rodriguez OA, Lowry CA, 2018 Acute administration of the nonpathogenic, saprophytic bacterium, *Mycobacterium vaccae*, induces activation of serotonergic neurons in the dorsal raphe nucleus and antidepressant-like behavior in association with mild hypothermia. Cell Mol Neurobiol 38, 289–304. [PubMed: 29134419]

Silva RC, Gargaro AC, Brandao ML, 2004 Differential regulation of the expression of contextual freezing and fear-potentiated startle by 5-HT mechanisms of the median raphe nucleus. Behav Brain Res 151, 93–101. [PubMed: 15084425]

Smith DG, Martinelli R, Besra GS, Illarionov PA, Szatmari I, Brazda P, Allen MA, Xu W, Wang X, Nagy L, Dowell RD, Rook GAW, Rosa Brunet L, Lowry CA, 2019 Identification and characterization of a novel anti-inflammatory lipid isolated from Mycobacterium vaccae, a soil-derived bacterium with immunoregulatory and stress resilience properties. Psychopharmacology (Berl).

Sommershof A, Aichinger H, Engler H, Adenauer H, Catani C, Boneberg EM, Elbert T, Groettrup M, Kolassa IT, 2009 Substantial reduction of naive and regulatory T cells following traumatic stress. Brain Behav Immun 23, 1117–1124. [PubMed: 19619638]

Spannuth BM, Hale MW, Evans AK, Lukkes JL, Campeau S, Lowry CA, 2011 Investigation of a central nucleus of the amygdala/dorsal raphe nucleus serotonergic circuit implicated in fear-potentiated startle. Neuroscience 179, 104–119. [PubMed: 21277950]

VanElzakker MB, Dahlgren MK, Davis FC, Dubois S, Shin LM, 2014 From Pavlov to PTSD: the extinction of conditioned fear in rodents, humans, and anxiety disorders. Neurobiol Learn Mem 113, 3–18. [PubMed: 24321650]

Author Manuscript Author Manuscript Author Manuscript Author Manuscript

Zass LJ, Hart SA, Seedat S, Hemmings SM, Malan-Muller S, 2017 Neuroinflammatory genes associated with post-traumatic stress disorder: implications for comorbidity. Psychiatr Genet 27, 1–16. [PubMed: 27635478]

Zuany-Amorim C, Sawicka E, Manlius C, Le Moine AL, Brunet LR, Kemeny DM, Bowen G, Rook G, Walker C, 2002 Suppression of airway eosinophilia by killed *Mycobacterium vaccae*-induced allergen-specific regulatory T-cells. Nat Med 8, 625–629. [PubMed: 12042815]

Author Manuscript Author Manuscript Author Manuscript Author Manuscript

Highlights

1. Treatment with *Mycobacterium vaccae* NCTC 11659 does not influence fear acquisition.
2. Treatment *M. vaccae* enhances between-session fear extinction.
3. Treatment with *M. vaccae* enhances within-session fear extinction.

Author Manuscript Author Manuscript Author Manuscript Author Manuscript

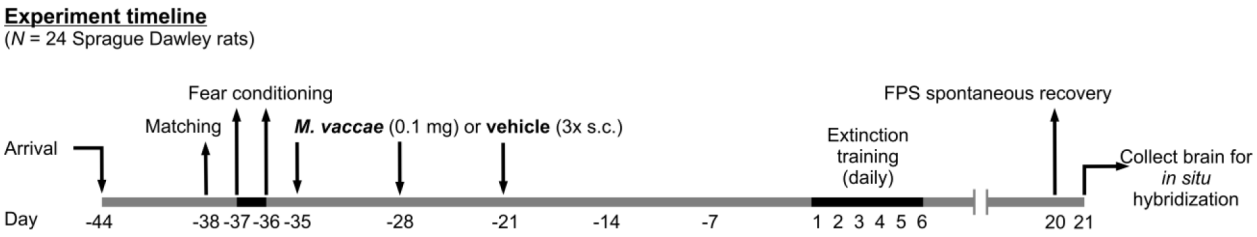

Figure 1.

Diagrammatic illustration of experimental design and timeline. Days 1 through 6 are defined as days that rats underwent fear-potentiated startle (FPS) extinction training. Sample sizes ($N = 24$, vehicle, $n = 12$; *M. vaccae*, $n = 12$). All animals ($N = 24$) were matched for assignment of treatment groups on Day −38. Rats received fear conditioning on Days −37 and −36 and received subcutaneous injections of either *M. vaccae* or vehicle once a week for three weeks (on days −35, −28, and −21). Day −1 is defined as the day before fear extinction training; Day 1 is defined as the first day of fear extinction training. Abbreviations: FPS, fear-potentiated startle; s.c., subcutaneous.

Author Manuscript Author Manuscript Author Manuscript Author Manuscript

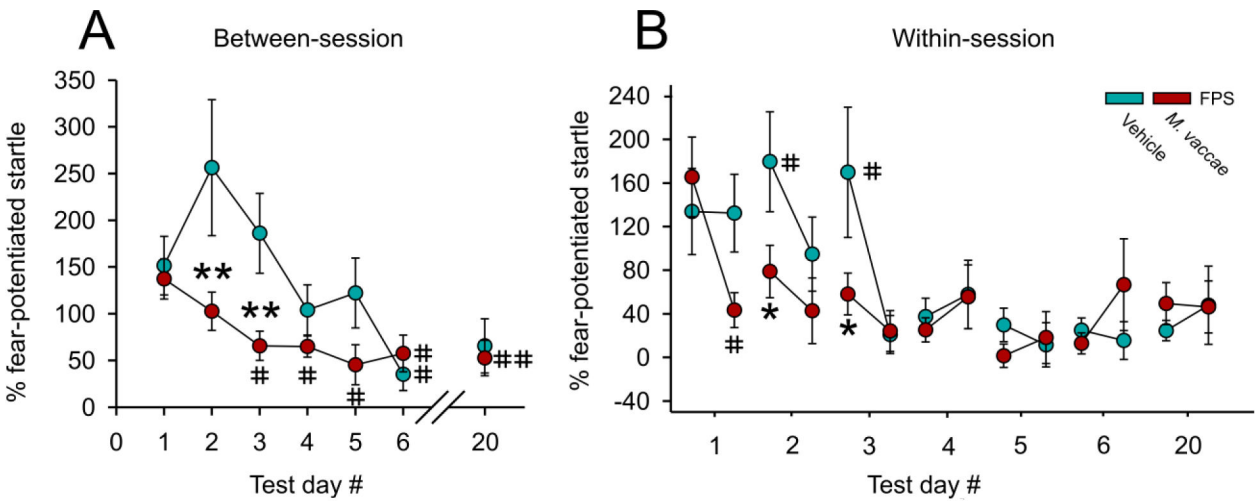

Figure 2.

M. vaccae prevents fear extinction resistance and enhances both between-session and within-session extinction of conditioned fear in male rats. (**A**) Between-session fear-potentiated startle (FPS) extinction, measured on Days 1-6 and spontaneous recovery of fear measured on Day 20, starting 36 days after fear conditioning (FPS extinction training). (**B**) Within-session extinction of conditioned fear measured on Days 1-6 and spontaneous recovery of fear, measured on Day 20. Data are presented as means ± standard error of means (SEMs). Data were analyzed using (A and B), linear mixed model (LMM) analysis with fixed effects of *M. vaccae* and day, with block nested within day; post hoc pairwise comparisons were made using Fisher's least significant difference (LSD) tests for between-subjects comparisons and paired *t*-tests for within-subjects comparisons. $^{*}p < 0.05$, $^{**}p < 0.01$, between-subjects effects; $^{\#}p < 0.05$, $^{\#\#}p < 0.01$, within-subjects effects. **A**) between-session fear extinction on Days 1-6, and spontaneous recovery of fear on Day 20; **B**) within-session fear extinction between the first 6 and last 6 (CS−/AS+) trials within the session. Sample sizes ($N = 24$, vehicle, $n = 12$; *M. vaccae*, $n = 12$).

Author Manuscript Author Manuscript Author Manuscript Author Manuscript

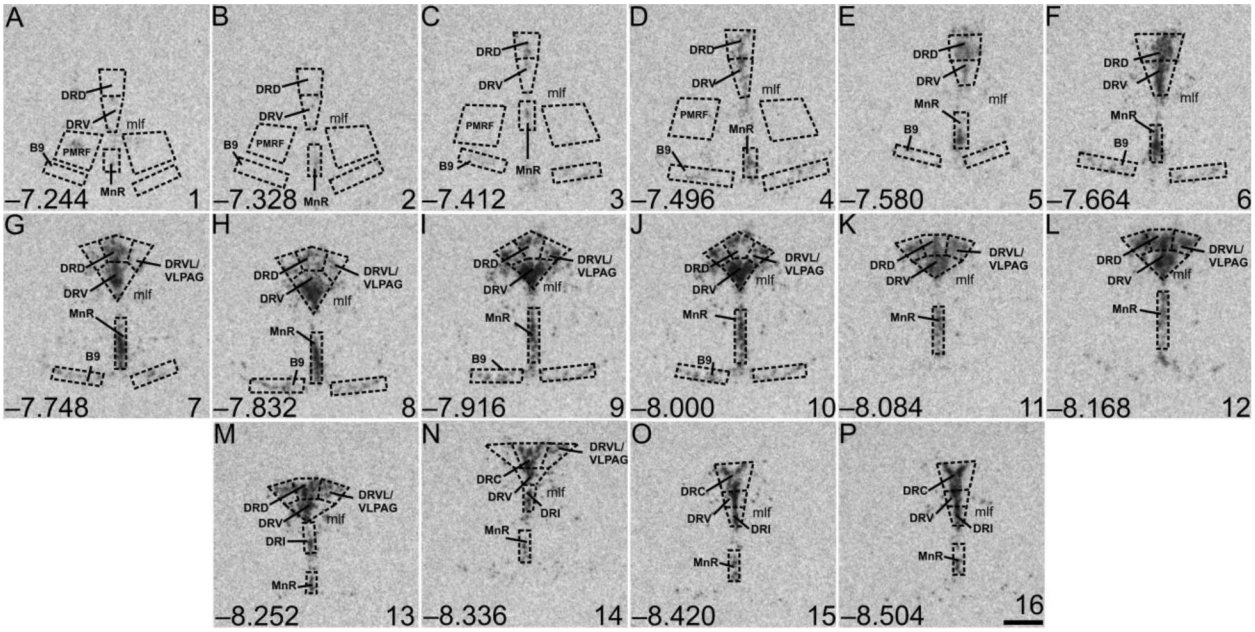

Figure 3.

Atlas of rat tryptophan hydroxylase 2 (*Tph2*) mRNA expression in the brainstem raphe complex (84 μm intervals) used for analysis of subregions of the dorsal raphe nucleus (DR), median raphe nucleus (MnR), B9 supralemniscal serotonergic cell group, and pontomesencephalic reticular formation (PMRF) with a high level of neuroanatomical resolution. Photographs are autoradiographic images of *Tph2* mRNA expression from a single rat in this study. The levels chosen for analysis ranged from (**A**) −7.244 mm bregma through (**P**) −8.504 mm bregma; bregma levels are listed in the lower left of each panel. Numbers in the lower right of each panel (1-16) correspond to rostrocaudal levels on the x-axis for Figure 4A and Supplemental Figure 1A-H. Dotted lines delineate different subdivisions of the DR, the MnR, B9 serotonergic cell group, and PMRF analyzed in this study, based on a stereotaxic atlas of the rat brain (Paxinos and Watson, 1998). Abbreviations: B9, supralemniscal serotonergic cell group; DRC, dorsal raphe nucleus, caudal part; DRD, dorsal raphe nucleus, dorsal part; DRI, dorsal raphe nucleus, interfascicular part; DRV, dorsal raphe nucleus, ventral part; DRVL/VLPAG, dorsal raphe nucleus, ventrolateral part/ventrolateral periaqueductal gray; mlf, medial longitudinal fasciculus; MnR, median raphe nucleus; PMRF pontomesencephalic reticular formation. Scale bar, 500 μm

Author Manuscript Author Manuscript Author Manuscript Author Manuscript

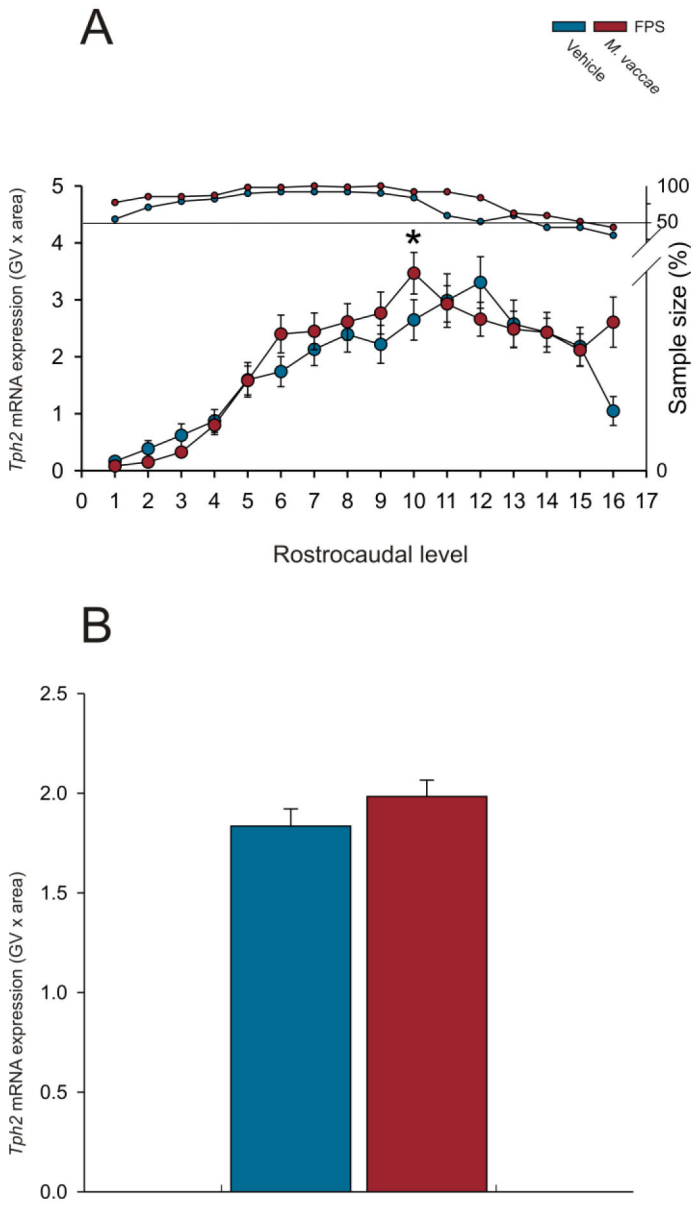

Figure 4.

Effects of repeated immunizations with a heat-killed preparation of *M. vaccae* or vehicle in rats exposed to fear conditioning, fear extinction, and spontaneous recovery on overall mean *Tph2* mRNA expression in the dorsal raphe nucleus (DR), median raphe nucleus (MnR), B9 supralemniscal serotonergic cell group, and pontomesencephalic reticular formation (PMRF). Each graph represents the mean (**A**) ± SEM or (**B**) + SEM of *Tph2* mRNA expression, i.e., (**A**) mean ± SEM of *Tph2* mRNA expression at each rostrocaudal level throughout the rostrocaudal extent of the DR, MnR, B9 supralemniscal serotonergic cell group, and PMRF. (**B**) Overall mean + SEM *Tph2* mRNA expression within the DR, MnR, B9 serotonergic cell group, and PMRF. Rats received fear conditioning on Days −37 and −36, followed by immunizations with a heat-killed preparation of *M. vaccae* or borate-buffered saline vehicle (Vehicle) on Days −35, −28, and −21, followed by fear extinction

Author Manuscript Author Manuscript Author Manuscript Author Manuscript

training on Days 1-6, and spontaneous recovery 14 days later (Day 20). Rats were euthanized 24 h later on Day 21. *$p < 0.05$, *M. vaccae* versus vehicle. Rostrocaudal levels 1 through 16 correspond to those illustrated in panels A-P of Figure 3.